Int J Fract (2010) 163:1–13
DOI 10.1007/s10704-010-9478-5

ORIGINAL PAPER

Rupture nucleation on an interface with a power-law relation between stress and displacement discontinuity

James R. Rice · Koji Uenishi

Received: 28 July 2009 / Accepted: 10 March 2010 / Published online: 2 April 2010

Abstract We consider rupture initiation and instability on a displacement-weakening interface. It is assumed to follow a power-law relation between a component of displacement discontinuity (whether tensile opening in mode I or shear slippage in modes II or III) and the reduction from peak strength of a corresponding component of stress (normal or shear stress) on the interface. That is, the stress decrease from peak strength, as the interface discontinuity develops, is assumed to be proportional to displacement-discontinuity to some exponent $n > 0$. The study is done in the 2D context of plane or anti-plane strain, for an initially coherent interface which is subjected to a locally peaked "loading" stress which increases quasi-statically in time. We seek to establish the instability point, when no further quasi-static solution exists for growth of the ruptured zone along the interface, so that dynamic rupture ensues. We have previously addressed the case of linear displacement-weakening ($n = 1$), and proven the remarkable result that for an unbounded solid, the length of the displacement-weakening zone along the interface at instability is universal, in the sense of being independent of the detailed spatial distribution of the locally peaked loading stress. Present results show that such universality does not apply when n differs from 1. Also, if $n < 2/3$, there is no phase of initially quasi-static enlargement of the rupturing zone; instead instability will occur as soon as the maximum value of the loading stress reaches the peak strength. We first employ an energy approach to give a Rayleigh–Ritz approximation for the dependence of quasi-static rupture length and maximum displacement-discontinuity on the loading stress distribution of a quadratic form. Results, depending on curvature of the loading distribution, show that qualitative features of the displacement-discontinuity development are significantly controlled by n, with the transition noted at $n = 2/3$. Predictions of the simple energy approach are in reasonable quantitative agreement with full numerical solutions and give qualitative features correctly.

Keywords Fracture nucleation · Interface failure · Cohesive zone model · Nonlinear displacement-weakening · Fault rupture nucleation · Nonlinear slip-weakening · Nucleation zone size

Koji Uenishi—Formerly at Department of Earth and Planetary Sciences and School of Engineering and Applied Sciences, Harvard University.

J. R. Rice (✉)
Department of Earth and Planetary Sciences
and School of Engineering and Applied Sciences,
Harvard University, 29 Oxford Street,
Cambridge, MA 02138, USA
e-mail: rice@seas.harvard.edu

K. Uenishi
Research Center for Urban Safety and Security,
Kobe University, 1-1 Rokko-dai, Nada,
Kobe 657-8501, Japan
e-mail: uenishi@kobe-u.ac.jp

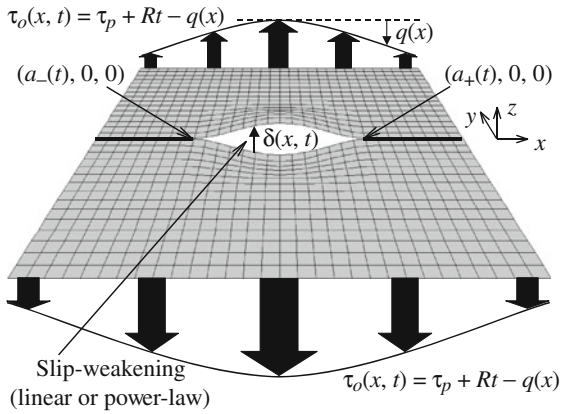

Fig. 1 A displacement field, associated with anti-plane shear (mode III) rupture in an infinite, homogeneous, isotropic, linear elastic solid, is schematically shown. The nonuniform loading stress $\tau_o(x, t)$ is locally peaked in space and changes gradually with time, at rate R. Inside the slipping region, a linear or power-law slip-weakening relation holds. The corresponding in-plane shear (mode II), or tensile (mode I) rupture problems can be defined analogously

1 Introduction

In previous study, Uenishi and Rice (2003) investigated the behaviors of displacement-weakening interfaces, specifically in the case of slip-weakening faults, and evaluated the nucleation length that is relevant to fault instability, i.e., earthquake nucleation, in that model. In the analysis, the case of a linear slip-weakening constitutive law

$$\tau\,(\delta) = \tau_p - W\delta, \tag{1}$$

(τ is shear stress, δ is slip, τ_p and W are positive constants) was mainly studied in the framework of two-dimensional quasi-static elasticity. They considered, in an infinite, homogeneous, isotropic elastic space, a planar fault under a locally peaked nonuniform loading stress, which is assumed to gradually change in time due to, for instance, tectonic loading, but to retain its peaked character in space (Fig. 1). Such nonuniform, locally peaked stress distribution may be expected, for example, as a result of residual stressing from prior seismic events, and is given mathematically (for the case of a fixed residual stress distribution) by

$$\tau_o\,(x, t) = \tau_p + Rt - q\,(x)\,. \tag{2}$$

Here, the fault plane coincides with the $x - z$ plane ($y = 0$) of a Cartesian coordinate system xyz, Rt is the stress change from that for which the peak in the loading stress distribution equals the shear strength of the fault, τ_p. At this peak strength τ_p, slip and weakening initiate. The function $q(x)$, which gives the exact shape of the loading stress distribution as a function of the position on the fault, x, satisfies $q(x) > 0$ for $x \neq x_p$ and $q(x_p) = 0$. Thus $t = 0$ is the time when the peak value of loading stress, at x_p, first reaches τ_p so that slip initiates at that point and then the slipping region $a_-(t) < x < a_+(t)$ expands quasi-statically. In Uenishi and Rice (2003) it was assumed that a linear slip-weakening law with constant weakening rate W ($W > 0$) applies at least approximately for the range of slips which occur prior to instability. We will make an analogous assumption for the power-law relations to be studied here. It was shown in that linear case that the size of the slipping region on a fault grows under increased loading stress until finally a critical nucleation length h_n is reached at which no further quasi-static solution exists. This marks the onset of a dynamically controlled instability. Such nucleation length h_n was analytically proven to be universal, i.e., independent of the exact shape of the loading stress distribution $q(x)$, and it is given by

$$h_n \approx 1.158\mu^*/W. \tag{3}$$

Here the numerical factor (to that many digits) comes from the least eigenvalue of a certain homogeneous problem. Also, $\mu^* = \mu$ (shear modulus) for mode III, and $\mu/(1-\nu)$ for mode II, with ν being Poisson's ratio. The same results apply, as do the new ones to be derived in the current presentation based on power-law displacement-weakening, for interfaces loaded in tension (mode I), in which case τ is to be reinterpreted as tensile stress, δ as opening displacement, and $\mu^* = \mu/(1-\nu)$. For a specific focus, we phrase much of the paper in terms of slip-weakening on a fault surface, recognizing that the results apply without change to nucleation of fracture under tensile loading of a displacement-weakening interface.

While the methodology of the paper, as presented in Appendices A, B and C, could be applied to any slip-weakening law $\tau = \tau(\delta)$ of interest, we here focus exclusively on cases for which the strength τ can be assumed to be given by

$$\tau\,(\delta) = \tau_p - A\delta^n, \tag{4}$$

for all slips δ experienced. Here A is a positive constant with units [stress/length^n], and n is also a positive constant (Fig. 2). We study slip development and its stability or instability for such a power form (as already

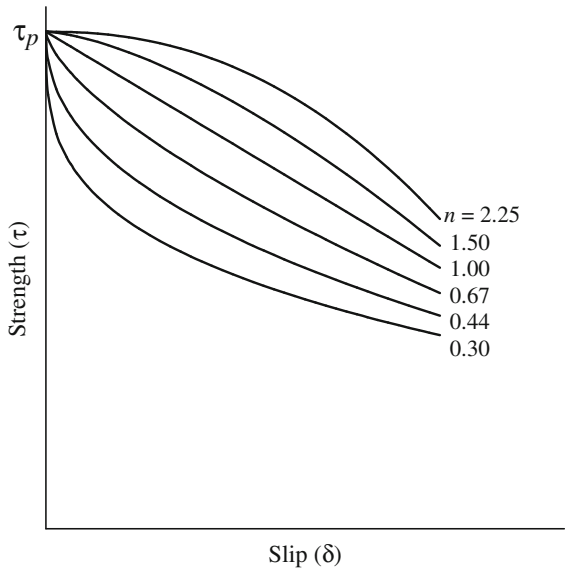

Fig. 2 The nonlinear, power-law slip-weakening constitutive relation. The fault strength τ is given by $\tau = \tau_p - A\delta^n$, where A and n are positive constants. The initial gradient of the curve, $d\tau/d\delta(\delta = 0^+)$, is zero when $n > 1$. It is a constant $[-A(< 0)]$ if $n = 1$ (linear case) and negative infinite $(-\infty)$ if $n < 1$

partly analyzed using dimensional analysis in Uenishi and Rice (2003)). First we employ an energy approach like in Rice (1992) and Rice and Beltz (1994) to give a Rayleigh–Ritz type approximation for the dependence of slipping zone length, and maximum slip, on the level and shape of the loading stress distribution (see "Appendices A and B" for the detailed description of the analytical method). A second approach is to provide a full numerical solution for the slip development (see Appendix C for the numerical methodology). Remarkably, the predictions of the simplified energy approach are in reasonable quantitative agreement with the full numerical solution, and predict qualitative features correctly.

It should be noted that the objective in this study is to show the mathematical properties of more generalized displacement-weakening interfaces under spatially nonuniform loading, simply because the displacement-weakening concept is widely used in fracture analysis. That includes cases of earthquake nucleation in seismology, although we do not intend here to support or advocate the use of slip-weakening laws in that context, as opposed to more elaborate laboratory-based descriptions of the rate and state type (Dieterich 1979; Ruina 1983). For studies of nucleation in the rate and state context, see Dieterich (1986, 1992), Tse and Rice (1986), Dieterich and Kilgore (1996), Lapusta and Rice (2003), Rubin and Ampuero (2005), and Ampuero and Rubin (2008). Similarly, studies of dynamic rupture based on thermally-driven fault weakening during seismic slip, with an essential dependence on slip rate, reveal responses such as self-healing rupture modes (Nodaet et al. 2009) which cannot be fully explained in the slip-weakening context. That stated, a recent study (Abercrombie and Rice 2005) has used seismological observations, interpreted to give seismic moment, radiated energy, and rupture duration, for earthquakes over a broad range of moment magnitude, M_w = 0.5 to 7.3, to constrain how shear stress τ varies with slip δ during seismic rupture, for slips ranging from ~0.2 mm to ~3 m. The measured data does not fully suffice for that, even in principle; Abercrombie and Rice (2005) noted that to infer a $\tau(\delta)$ relation one must make an assumption, not testable through seismic observations of the type mentioned, about how the final static τ at a point along the fault, well after rupture arrest, relates to the τ at the same point just before arrest of sliding. They reported results for the case for which the two τ are the same, although theoretical studies (Madariaga 1976; Nodaet et al. 2009) have identified cases for which the τ just before slip arrest may be greater or less than the final static τ. In that way, they found that the results for δ ranging from 0.2 mm to 0.2 m could be fit approximately (with large scatter) by a relation in the form of Eq. (4) with $n \approx 0.3$, although re-examination shows that results for δ ranging from 1 to 10 mm are better described by Eq. (4) with $n \approx 0.7$.

2 Nonlinear displacement-weakening

2.1 Analysis based on the simplified energy approach

Consider a nonlinear power-law slip-weakening constitutive relation given by Eq. (4). Assume, for simplicity, that the loading stress falls off from its locally peaked value with a quadratic dependence (with curvature κ [stress/length^2] (> 0)) on distance x from the peak location, at $x = 0$, *as* $q(x) = \kappa\, x^2/2$ for small x. Then, the slipping region expands symmetrically ($a_+ = -a_- \equiv a$), and Eqs. (B5, B6) and (B8) in Appendix B imply, as briefly mentioned in Rice and Uenishi (2002) and Uenishi and Rice (2003), that the critical length $h_n =$

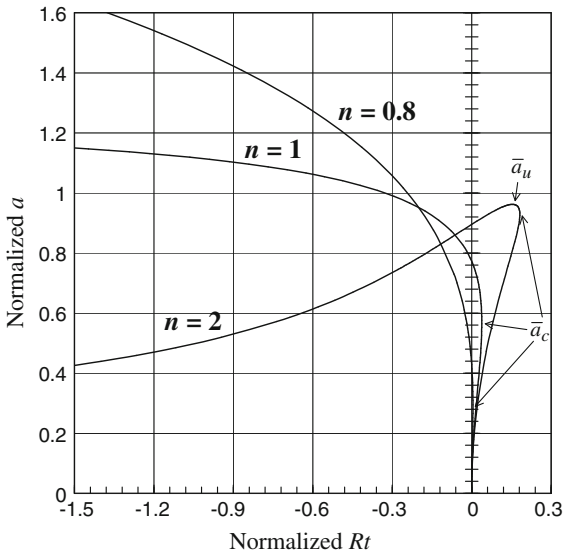

Fig. 3 Relation between the half-length a (shown non-dimensionally, with *overbar*) of the slipping region and the stress change Rt for $n > n_{th}(= 2/3)$. Note that in all cases a maximum value of load Rt occurs along the loci of equilibrium solutions shown, and we denote by a_c the corresponding half-length at instability. The behavior is qualitatively similar to that for the linear case ($n = 1$). Slip develops gradually with increasing remote loading until the slipping zone reaches the critical length. For $n > 1$, however, the unstable equilibrium range of the results (commencing at a_c and the maximum possible loading Rt) exhibits a maximum value for a, labelled a_u, marking the start of a nonphysical branch (see text)

$2a$ at instability depends on the curvature κ of the loading stress distribution when the slip-weakening relation is not linear, i.e., $n \neq 1$. In other words, there is no longer a universal nucleation length that is independent of κ. The analysis in "Appendix B" also shows that qualitative features of the slip development are significantly controlled by the power, n, of the slip-weakening law (4). In the following sections, we will discuss qualitatively the mathematical features for the three distinctive ranges of n, namely $n > n_{th}$, $n = n_{th}$ and $0 < n < n_{th}$, where $n_{th} = 2/3$ is the threshold value. The results obtained by the simplified energy approach will be shown in the normalized form (using Eqs. (B11) or (B19) depending on the power n).

2.2 The case $n > n_{th}(= 2/3)$

Figure 3, for three different values of $n > 2/3$, namely for $n = 0.8$, 1 and 2, shows that the behavior is qualitatively similar to that for $n = 1$ (linear case), in that the slipping region (represented by the half-length of the region, a, and shown in a non-dimensional form) first develops gradually with increasing remote loading Rt [that is, $d(Rt)/da > 0$ near $a = 0^+$, as confirmed by Eq. (B7)]. That occurs until a reaches the critical length a_c. As $a \to a_c$, $da/d(Rt) \to \infty$, so that $d(Rt)/da \to 0$, corresponding to a maximum in sustainable load under the assumed equilibrium conditions. Beyond that critical length $2a_c$, an unstable equilibrium branch commences for which the load must decrease to continue to grow the length of the slipping region under the assumed equilibrium conditions [$d(Rt)/da < 0$ for sufficiently large a in Eq. (B7)]. When discussing such unstable equilibrium solutions, we suspend thinking of t as time, and simply interpret Rt as the level of uniform tectonic loading in Eq. (2), and Fig. 1, which would allow an unstable equilibrium configuration of length $2a$.

The system must become unstable at that critical length a_c, and corresponding load Rt, because as shown by the results in Fig. 3, there is no equilibrium solution for larger values of the load Rt. Hence, in the situation of a continuous slow increase in load Rt, the rupture should transition into an initially-controlled dynamic process at greater load.

If $n > 1$, as shown in Fig. 3, along the unstable equilibrium branch starting at half-length a_c and corresponding load Rt (the maximum possible load for equilibrium), $da/d(Rt)$, which turned negative at a_c, can pass through zero at a half-length denoted $a = a_u$, beyond which $da/d(Rt)$ resumes positive values. Equation (B15) confirms the expected result that $a_u > a_c$ always. We can attribute no physical significance to this branch commencing at a_u, beyond which $da/d(Rt)$ resumes positive values, because under conditions of continuous quasistatic increase in load the system will have already gone unstable at a_c. Also, to trace out that range beginning at a_u would require an unphysical direction of traversal of the slip-weakening relation, with material along the ruptured surface going from weakened to strong again. Therefore, the branch of unstable equilibrium states must be understood to exist only between the half-lengths a_c and a_u.

2.3 The case $n = n_{th}(= 2/3)$

In this case, the loading stress must either always increase, or stay constant, or always decrease in order

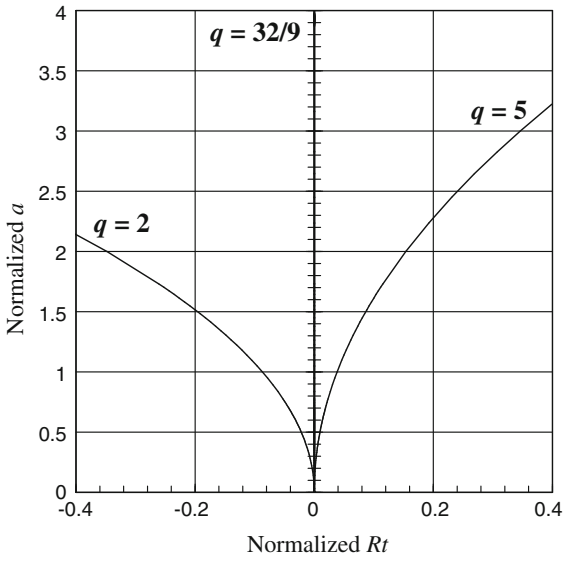

Fig. 4 The a versus Rt relation for $n = n_{th}(= 2/3)$: The loading stress must in this case either always increase, or stay constant, or always decrease in order to expand the slipping region. A dimensionless parameter q ($\equiv \kappa\mu^{*2}/A^3$) controls the character of this slip response

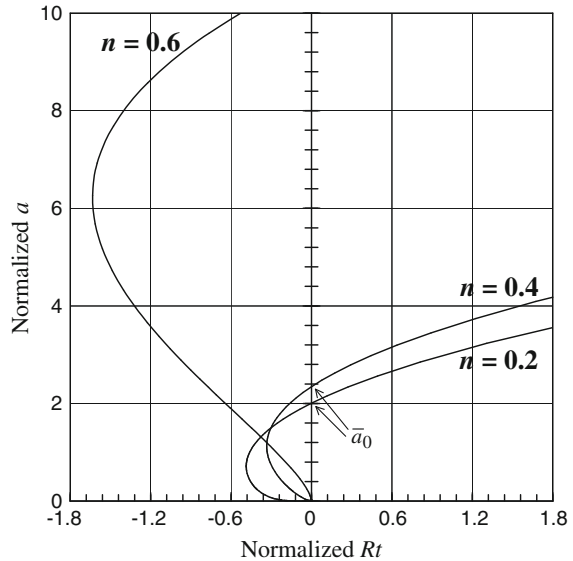

Fig. 5 Relationship between the half of the slipping length a and the stress change Rt for $0 < n < n_{th}(= 2/3)$. Upon initiation of slip the loading Rt must be decreased in order to quasi-statically expand the slipping region

to expand the slipping region. Whichever occurs is controlled by the dimensionless parameter $q = \kappa\mu^{*2}/A^3$, a measure of the curvature of the loading stress distribution, and not to be confused with the function $q(x)$ in Eq. 2 and Fig. 1. That parameter has a critical value of $q_c = 32/9$ (Fig. 4): (a) If $q < q_c$, slip development is always unstable, i.e., the remote loading must be decreased in order to widen the slipping region; (b) If $q > q_c$, the slip development is always stable (remote loading must be increased); (c) If $q = q_c$, the slipping region can take any length without change of the remote loading. The physical meaning of this threshold value n_{th} will be discussed in Sect. 3.1.

2.4 The case $0 < n < n_{th}$ (= 2/3)

Figure 5 indicates that, if $n < 2/3$, upon initiation of slip the loading must be decreased in order to quasi-statically expand the slipping region (Eqs. (B5) and (B7) imply $d(Rt)/da < 0$ near $a = 0^+$). At $a = 0^+$, $d(Rt)/da = 0^-$ (the vertical axis, $Rt = 0$, is tangent to the curve) if $1/2 < n < 2/3$, but $d(Rt)/da = -\infty$ (the horizontal axis is tangent to the curve) if $0 < n < 1/2$. That is, an unstable equilibrium branch initiates at slip $\delta = 0^+$, and hence instability will occur as soon as the peaked value of the loading stress reaches the strength τ_p. This is a prediction based on using the power-law starting at $\delta = 0^+$.

In this $n < 2/3$ range, the unstable equilibrium branch ultimately stabilizes with increasing slipping length, in that the loading must start to increase again to grow the slipping region further ($d(Rt)/da > 0$ for sufficiently large a). That may imply that as soon as the peak of loading reaches the strength τ_p of the fault, the slipping region nucleates and then expands to a finite size at which arrest occurs at $a = a_0$ (mathematically given by Eq. (B13), if the dynamic effect can be ignored. Note, however, that the predicted re-emergence of equilibrium solutions at finite a results from an analysis in which, because of the $q(x)$ term in Eq. (2), the loading stress decreases quadratically with distance x and even turns negative at sufficiently great x. We do not expect such pop-in to an equilibrium configuration, i.e., fracture arrest, to occur when the loading stress remains comparable to, if less than, τ_p at all x, rather than diminishing towards zero and reversing sign as in the analysis presented. That is, we suspect that it is a simple artifact of the pre-stress being negative away from the point of peak loading, but have not done analysis to confirm that.

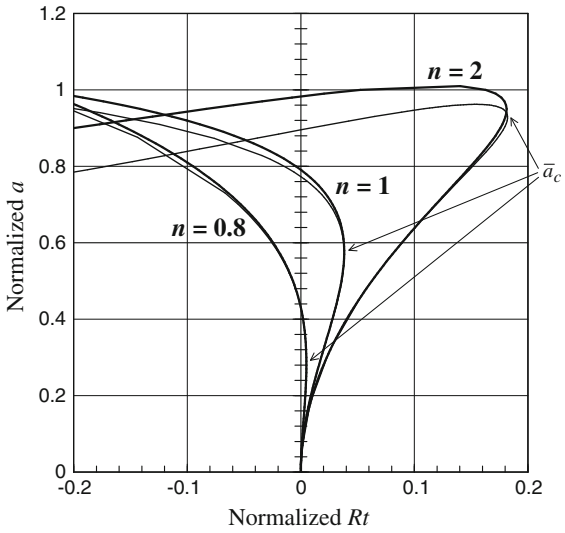

Fig. 6 Comparison of the numerical (*thick lines*) and the simplified analytical (*fine lines*) results, showing the relation between the half-length a and the stress change Rt for $n > n_{th}$

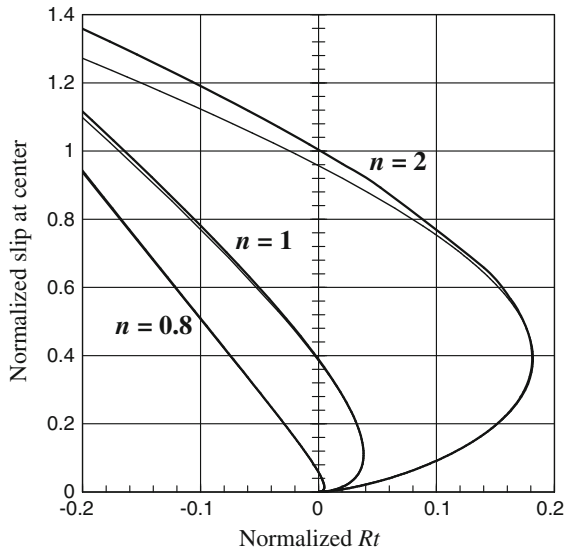

Fig. 7 The numerical (*thick lines*) and the simplified analytical (*fine lines*) results. The relation between the slip $\delta(x = 0)$ at the center of the slipping region and the stress change Rt is shown for $n > n_{th}$

2.5 Numerical approach

Alternatively, a numerical approach has been taken, to solve within given accuracy the exact statement of the problem in Eq. (C1), i.e., without the apriori assumption of a functional form for the slip distribution, like adopted in Eq. (A8) for use in the simplified energy approach. The numerical procedure is described in "Appendix C", and results of it are used to examine the accuracy of the approximate analytical solutions, underlying results shown in the previous sections. We have set the allowable error $\varepsilon = 1 \times 10^{-8}$ ("Appendix C") in the numerical calculations, and in all diagrams, we normalize the position-related variables (a and x), stress change (Rt) and slip (δ) as before (Eqs. (B11) or (B19) depending on n).

The numerically obtained results are shown in Figs. 6, 7, 8 and 9. In generating these diagrams, we set the normalized grid spacing $\overline{\Delta x}$ as 0.01 for $n \geq 0.8$, 0.08 for $n = 0.6$, 0.03 for $n = 0.4$ and 0.015 for $n = 0.2$. Figures 6 and 8 indicate the relation between the half-length a of the slipping region and the stress change Rt while Figs. 7 and 9 show the slip development at the center of the slipping region (D in the analytical case; see Eq. (A8)). In all Figs. 6, 7, 8 and 9, the numerical results (thick lines) and the simplified analytical ones (fine lines) show good agreement when $\bar{a} \leq \bar{a}_c$ (i.e., up to the instability point

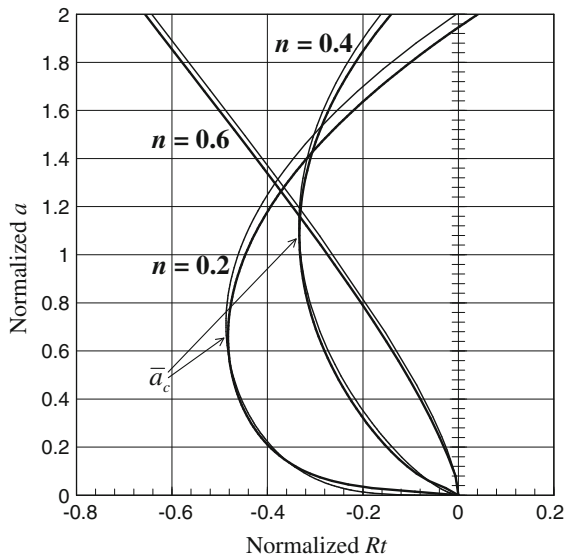

Fig. 8 The numerical (*thick lines*) and the analytical (*fine lines*) results showing the relation between the half-length a and the stress change Rt for $0 < n < n_{th}$

point at which $d(Rt)/da$ and $d(Rt)/d\delta(x = 0)$ become zero). For example, for $n = 0.4$, both analytical and numerical calculations indicate that $\overline{Rt} \approx -0.334$ at $\bar{a} = \bar{a}_c \approx 1.1$ (Fig. 8). The difference between the numerical and the analytical results is not negligible for larger values of $\bar{a}$, especially with very large or very

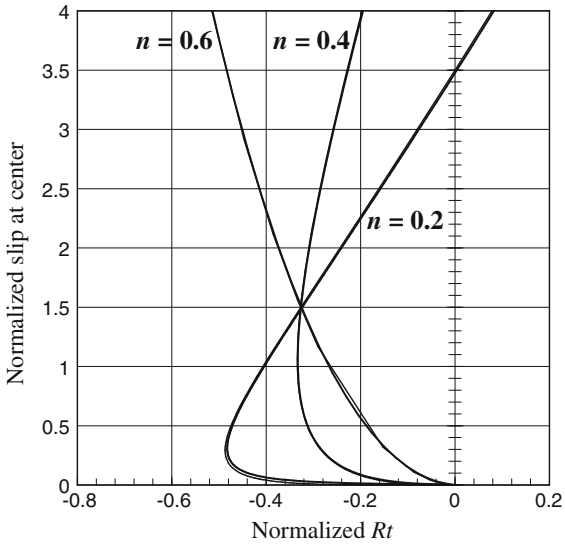

Fig. 9 The numerical results (*thick lines*) and the analytical ones (*fine lines*) indicating the relation between the slip $\delta(x = 0)$ at the center of the slipping region and the stress change Rt for $0 < n < n_{th}$

small values of n. For $n = 0.2$ (Fig. 8), when $\overline{Rt} = 0$, the numerical simulation gives $\bar{a} = 0$ and 1.95 while the analysis renders $\bar{a} = 0$ and 2.01 ($= \bar{a}_0$ in Eq. (B14), showing approximately 3% difference. However, the general qualitative features observed in the simplified energy approach, described in the last three sections, are reproduced also in the more exact numerical results, including the special case of $n = n_{th}$.

3 Discussion

3.1 Threshold value of the power, n_{th}

We have found that the qualitative features of the slip-weakening fault vary considerably, depending on whether the power n of the slip-weakening law (4) is larger than the threshold or not. For the quadratic loading function $q(x) = \kappa x^2/2$, the threshold value is $n_{th} = 2/3$. Physically, this value corresponds to the situation where the energy U of the slip-weakened body changes monotonically or remains the same as the remote loading changes with Rt: When the dimensionless parameter $q = q_c (= 32/9)$, the energy U is always equal to the energy when there is no slip, U_o, i.e., $U = U_o$, regardless of the length of the slipping region, and therefore the half-length a can take any value without change of Rt; If $q > q_c$, the energy U always decreases, $U < U_o$, as the slipping region on the fault stably expands with Rt; If $q < q_c$, then $U > U_o$ and $Rt < 0$, suggesting unstable slip development on the fault.

This threshold $n_{th} = 2/3$ can be obtained also from dimensional analysis (Uenishi and Rice 2003) and its value is independent of the curvature κ of the loading, if $\kappa > 0$. However, if the stress distribution $q(x)$ is given in a more general form like $q(x) = \kappa x^m/m$ (m even integer (>0)), n_{th} varies depending on the power m and is written as

$$n_{th} = m/(m+1) \text{ for } q\,(x) \\ = \kappa x^m/m.\ (m \text{ even integer } (>0)) \quad (5)$$

Now the dimension of κ is [stress/length^m], and except for the adjustment associated with this change of dimension, the general mechanical characteristics of the slip-weakening fault, i.e., the behaviors for the three cases, $n > n_{th}$, $n = n_{th}$ and $0 < n < n_{th}$, remain the same for different values of m. (Of course, the case $m = 2$, for which $n_{th} = 2/3$, pertains to any loading stress distribution with an analytic maximum, with positive downward curvature at the peak-loaded point.)

4 Conclusions

We studied slip development and its stability or instability for a power-law slip-weakening fault. In addition to the result that when the power n is different from 1, there is no longer a universal nucleation length, independent of the curvature of the loading stress distribution, both the simplified energy approach and the numerical calculations show that qualitative features of the slip development are considerably controlled by n.

Principal results are as follows: (1) If $n > n_{th} (= 2/3)$, the behavior is qualitatively similar to that for $n = 1$ (linear case) of Uenishi and Rice (2003). Slip develops gradually with increasing remote loading until it reaches the critical length above which no stable solution for increased loading exists. (2) The case $n = n_{th}$ is transitional. The loading stress must in that case either always increase, or stay constant, or always decrease in order to expand the slipping region. Whichever occurs is controlled by a dimensionless parameter. (3) If $0 < n < n_{th}$, the analysis indicates that upon slip initiation

the loading must be decreased in order to quasi-statically expand the slipping region, suggesting instability at zero slip and the lack of any finite-size nucleation zone.

Acknowledgments This study was supported by the Southern California Earthquake Center which is funded by Cooperative Agreements NSF-EAR 0106924 and USGS 02HQAG0008 (this is SCEC contribution number 1409), and by funding for K.U. from the Japanese Society for the Promotion of Science.

Appendix A Simplified energy approach

Based on an energy approach (Rice 1992; Rice and Beltz 1994), we discuss the approximate behavior of the slip development on a slip-weakening fault. This approach can be applied also to the analysis of three-dimensional fault rupture, e.g., with assumed nucleation zones of circular or elliptical plane form (Uenishi and Rice 2004, manuscript to be submitted, 2010). We employ the Cartesian coordinate system xyz in our analysis.

A1 Basic concepts

We define the functional $M[\delta(\mathbf{x})]$ as the reduction in stress, from some initial distribution $\tau_o(\mathbf{x})$ to an altered distribution $\tau(\mathbf{x})$, on the fault plane ($y = 0$) due to the introduction of slip $\delta(\mathbf{x})[\mathbf{x} = (x, z)]$, and express it as

$$\tau\,(\mathbf{x}) - \tau_o\,(\mathbf{x}) = -M\,[\delta\,(\mathbf{x})]\,. \tag{A1}$$

For two-dimensional plane strain conditions in an infinite, isotropic and homogeneous elastic solid with the slipping region $a_- < x < a_+$, it is given by the standard continuous distribution of line dislocations, as (e.g., Bilby and Eshelby 1968)

$$M[\delta(x)] = \frac{\mu^*}{2\pi}\int_{a_-}^{a_+}\frac{d\delta(\xi)/d\xi}{x-\xi}d\xi, \tag{A2}$$

where, as in the main text, $\mu^* = \mu$ (shear modulus) for mode III and $\mu/(1-\nu)$ for modes I and II, with ν being Poisson's ratio. (We use the notation $M[\delta(\mathbf{x})]$ for conciseness but it would be more precise to rewrite M as $M[\delta(\xi), -a_- < \xi < a_+](x)$ to emphasize that it is a function of x, which is a functional of $\delta(\xi)$ on the given interval.) The change $s[\delta(\mathbf{x})]$ in elastic energy of the system outside the slipping region due to introduction of δ, is given by

$$\begin{aligned} s\,[\delta\,(\mathbf{x})] &= -\frac{1}{2}\int_S [\tau_o(\mathbf{x}) + \tau\,(\mathbf{x})]\delta(\mathbf{x})dS \\ &= \frac{1}{2}\int_S M[\delta(\mathbf{x})]\delta(\mathbf{x})dS - \int_S \tau_o(\mathbf{x})\delta(\mathbf{x})dS, \end{aligned} \tag{A3}$$

where S is the area of slipping region.

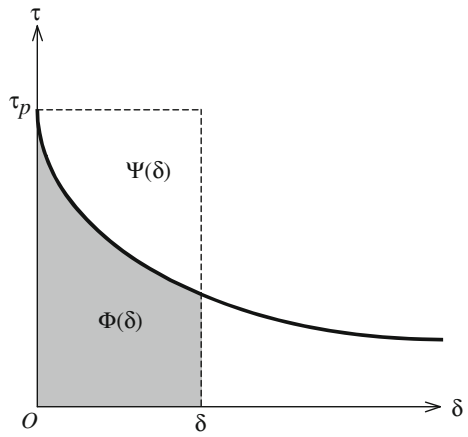

Fig. 10 A general displacement-weakening constitutive law is shown where the area under the τ versus δ curve between $\delta = 0$ and $\delta = \delta$, $\Phi(\delta) \equiv \int_0^\delta \tau(\eta)d\eta$, is the displacement-weakening energy per unit area of the failing interface (the concept of "energy" can be used for a frictionally weakening or failing interface in cases for which $d\delta/dt$ is always ≥ 0). The complementary energy per unit area of the interface is given by the area $\Psi(\delta) \equiv \tau_p\delta - \Phi(\delta)$

Here, a general displacement-weakening constitutive law is assumed (Fig 10), giving τ as a function of δ. For real slip-weakening (or, in mode I, for real tensile decohesion), τ can be regarded as a function of δ, for $\delta > 0$, only for cases in which there is no unloading from states along the displacement-weakening curve. Our analysis is physically relevant only for that situation, and for it we can treat the failing interface as if it was "elastic" in the sense of exhibiting a τ which is a unique function of δ. In such cases, an energy per unit area of the slip plane, $\Phi(\delta)$, can be defined by

$$\Phi\,(\delta) = \int_0^\delta \tau(\varsigma)d\varsigma$$

$$= \tau_p \delta - \int_0^{\delta} [\tau_p - \tau(\varsigma)] d\varsigma$$
$$\equiv \tau_p \delta - \Psi(\delta), \tag{A4}$$

where $\Psi(\delta)$ is the complementary energy per unit area of slip plane.

We define U_o as the energy when there is no slip, i.e., when $\delta(\mathbf{x}) = 0$ everywhere on the fault plane. Then, the energy functional $U[\delta(\mathbf{x})]$ of the slip-weakened body with the slip distribution $\delta(\mathbf{x})$ is the sum of U_o, the energy change of the system outside the slipping region due to introduction of slip $\delta(\mathbf{x})$, and the energy of the slip plane due to $\delta(\mathbf{x})$. Mathematically, it is expressed as

$$U[\delta(\mathbf{x})] = U_o + s[\delta(\mathbf{x})] + \int_S \Phi[\delta(\mathbf{x})] dS$$
$$= U_o + \frac{1}{2} \int_S M[\delta(\mathbf{x})] \delta(\mathbf{x}) dS$$
$$- \int_S \tau_o(\mathbf{x}) \delta(\mathbf{x}) dS + \int_S \Phi[\delta(\mathbf{x})] dS. \tag{A5}$$

At equilibrium U must be stationary, i.e., if Δ denotes an infinitesimal variation, $\Delta U = 0$ (to first order) for arbitrary variations of the slip distribution.

For the two-dimensional case, defining Rt as in the text so that the peak of the remote loading is τ_p at $Rt = 0$, we have

$$\tau_o = \tau_p + Rt - q(x) \quad \text{and}$$
$$\tau = \tau(\delta) \text{ within the slipping region.} \tag{A6}$$

Then, making U the energy per unit distance perpendicular to the x-y plane,

$$U[\delta(x)] = U_o + \frac{1}{2} \int_{a_-}^{a_+} M[\delta(x)] \delta(x) dx$$
$$- \int_{a_-}^{a_+} [\tau_p + Rt - q(x)] \delta(x) dx$$
$$+ \int_{a_-}^{a_+} \Phi(\delta(x)) dx$$
$$= U_o + \frac{1}{2} \int_{a_-}^{a_+} M[\delta(x)] \delta(x) dx$$
$$- \int_{a_-}^{a_+} [Rt - q(x)] \delta(x) dx - \int_{a_-}^{a_+} \Psi(\delta(x)) dx. \tag{A7}$$

At equilibrium, $\Delta U = 0$ for arbitrary variations $\Delta\delta$, Δa_+ and Δa_-. It is not difficult to see that this re-creates equilibrium equations with singularity-free ends at $x = a_\pm$ (see Uenishi and Rice 2003).

A2 Application to slip-weakening nucleation by symmetrically peaked loading

In this section, slip development under symmetrically peaked loading is considered in the two-dimensional context. The slipping region expands also symmetrically, i.e., $a_+ = -a_-(\equiv a)$ if the position for the peak of the remote loading is set at $x = 0$. We further assume, as an approximate form, a one-degree-of-freedom representation of slip

$$\delta(x) = D(a^2 - x^2)^{3/2}/a^3, \quad (-a < x < +a) \tag{A8}$$

which induces no stress singularity at ends ($x = \pm a$). Here, D is a constant that represents the maximum slip, occurring at at $x = 0$. Then, the functional $M[\delta(x)]$ is given by

$$M[\delta(x)] = \frac{3\mu^* D}{2\pi a^3} \int_{-a}^{+a} \frac{\xi \sqrt{a^2 - \xi^2}}{\xi - x} d\xi$$
$$= \frac{3\mu^* D}{2a} \left(\frac{1}{2} - \frac{x^2}{a^2} \right), \quad -a < x < +a \tag{A9}$$

and the energy functional U of the slip-weakened body is

$$U = U_o + \frac{3\pi}{32} \mu^* D^2 - [\beta Rt - Q(a)] aD$$
$$- a \int_{-1}^{+1} \Psi\left(D(1 - u^2)^{3/2} \right) du. \tag{A10}$$

Here, we have defined $u \equiv x/a$, $\beta \equiv \int_{-1}^{+1} (1 - u^2)^{3/2} du (= 3\pi/8)$ and $Q(a) \equiv \int_{-1}^{+1} q(au)(1 - u^2)^{3/2} du$.

Since $\Delta U = 0$ for any ΔD and Δa, we obtain the following equations

$$\frac{\partial U}{\partial a} = -[\beta Rt - Q(a) - aQ'(a)]D - \int_{-1}^{+1} \Psi\left(D(1-u^2)^{3/2}\right) du = 0, \text{ and}$$
$$\frac{\partial U}{\partial D} = \frac{3\pi}{16}\mu^* D - [\beta Rt - Q(a)]a - a\int_{-1}^{+1} \Psi'\left(D(1-u^2)^{3/2}\right)(1-u^2)^{3/2} du = 0. \tag{A11}$$

From Eq. (A11), D and a can be determined in terms of Rt, and also D can be obtained as a function of a.

A3 Case of linear slip-weakening

In the case of the linear slip-weakening law (1), the complementary energy can be written as $\Psi(\delta) = W\delta^2/2$ and $\Psi'(\delta) = W\delta$ and hence, we have from Eq. (A11)

$$D = \frac{a^2 Q'(a)}{\frac{3\pi}{16}\mu^* - \frac{16}{35}aW} \quad \text{and}$$
$$\beta Rt = Q(a) + \frac{\frac{3\pi}{16}\mu^* - \frac{32}{35}aW}{\frac{3\pi}{16}\mu^* - \frac{16}{35}aW} aQ'(a). \tag{A12}$$

The critical half-length a_c ($= h_n/2$) of the slipping region at rupture instability can be obtained as the value of a when $d(Rt)/da \to 0$. For instance, for a symmetric, quadratic function $q(x) = \kappa x^2/2$ ($\kappa > 0$) for small x, we have $Q(a) = \rho\kappa a^2$ and the condition $d(Rt)/da = 0$ at $a = a_c$ gives

$$\frac{512}{245}\lambda^2 - \frac{54}{35}\pi\lambda + \frac{27}{128}\pi^2 = 0, \tag{A13}$$

where $\rho \equiv \frac{1}{2}\int_{-1}^{+1} u^2(1-u^2)^{3/2}du (= \pi/32)$ and $\lambda \equiv a_c W/\mu^*$. Solving Eq. (A13) renders the critical nucleation length h_n as

$$h_n = 2a_c = 2\lambda\mu^*/W \approx 1.138\mu^*/W. \tag{A14}$$

We compare this result with the exact one, Eq. (3), and notice that there is an error of only about 1.7% in this simplified energy approach.

Appendix B Nonlinear slip-weakening: simplified energy approach

Consider now the nonlinear slip-weakening constitutive relation given by the power-law, Eq. (4). Assume again that the remote loading can be approximately given with $q(x) = \kappa x^2/2 (\kappa > 0)$ for the sufficiently small x that we consider. For this quadratic loading, the slipping region expands symmetrically with the center located at $x = 0$ ($a_+ = -a_- \equiv a$). The equilibrium conditions (A11) for the slip distribution (A8), when we eliminate Rt so as to express a in terms of D, lead to

$$\frac{\sqrt{\pi}}{16}(3\mu^* D - \kappa a^3) - \frac{n}{n+1}\frac{\Gamma((3n+5)/2)}{\Gamma((3n+6)/2)} AaD^n = 0 \tag{B1}$$

where Γ is the gamma function. We define a dimensionless parameter P of the form

$$P \equiv C_1 AD^n/(\kappa a^2), \tag{B2}$$

where the dimensionless positive constant C_1, depending on n, is chosen such that the relation (B1) has the form

$$\mu^* D/(\kappa a^3) = (1/3) + P. \tag{B3}$$

The constant C_1 is given by

$$C_1 \equiv \frac{16}{3\sqrt{\pi}}\frac{n}{n+1}\frac{\Gamma((3n+5)/2)}{\Gamma((3n+6)/2)}, \tag{B4}$$

and Eq. (B3) can be rewritten as

$$Ca^{-(3n-2)/n}P^{1/n} = (1/3) + P \tag{B5}$$

where

$$C \equiv C_1^{-1/n}\kappa^{-(n-1)/n}\mu^* A^{-1/n} \tag{B6}$$

is dimensional. Note that Eq. (B5) implicitly defines P as a function of a. The relation for Rt can now be inferred from either of Eqs. (A11), giving for Rt and $d(Rt)/da$ the expressions

$$Rt = \kappa a^2(1 - 2P/n)/4, \quad \text{and}$$
$$\frac{d(Rt)}{d(\kappa a^2)} = \frac{1}{4}\frac{1 - 3nP - 3P^2}{1 + 3(1-n)P}. \tag{B7}$$

Equation (B7) shows that the critical condition for loss of equilibrium, $d(Rt)/da = 0$, is achieved when

$$P = P_c \equiv \sqrt{\frac{n^2 + (4/3)}{4}} - \frac{n}{2}. \tag{B8}$$

Since P is given implicitly in terms of a by Eqs. (B5, B7), gives the evolution of Rt with a, and Eq. (B8) gives the value of a when the evolution of a with Rt goes from stable to unstable, or vice versa. Also, setting $P = P_c$ in Eq. (B5), we obtain the value of $a = a_c$ at that transition

(if n is not the threshold value n_{th} (= 2/3); the value of a at the transition approaches either 0^+ or infinity as $n \to n_{th}$). Equations (B5, B6) and (B8) show when $n \neq 1$, that critical length a_c depends on the curvature κ of the loading stress distribution, i.e., there is no longer a universal nucleation length that is independent of κ.

In the following we will mathematically show the difference between the two cases, namely $n \neq n_{th}$ and $n = n_{th}$. At this stage, it may be convenient to define a new dimensionless load curvature parameter q, not to be confused with the function $q(x)$ of Eq. (2), as

$$q \equiv \kappa \mu^{*^{-(n-2)/n}} A^{-2/n}. \tag{B9}$$

B1 The case $n \neq n_{th}(= 2/3)$

For cases other than $n = 2/3$,

$$\begin{aligned} \kappa a^2 &= \mu^* C_1^{-2/(3n-2)} q^{n/(3n-2)} \\ &\quad \times [(1/3) + P]^{-2n/(3n-2)} P^{2/(3n-2)}, \\ Rt &= \kappa a^2 (1 - 2P/n)/4, \quad \text{and} \\ D &= [\kappa a^2 P/(C_1 A)]^{1/n}, \end{aligned} \tag{B10}$$

hold. With the normalized parameters

$$\begin{aligned} \bar{a} &\equiv \frac{A^{1/(3n-2)} a}{\kappa^{(1-n)/(3n-2)} \mu^{*n/(3n-2)}} = \frac{\kappa^{1/2} a}{\mu^{*1/2} q^{n/(6n-4)}}, \\ \overline{Rt} &\equiv \frac{A^{2/(3n-2)} Rt}{\kappa^{n/(3n-2)} \mu^{*2n/(3n-2)}} = \frac{Rt}{\mu^* q^{n/(3n-2)}}, \quad \text{and} \\ \bar{D} &\equiv \frac{A^{3/(3n-2)} D}{\kappa^{1/(3n-2)} \mu^{*2/(3n-2)}} = \frac{A^{1/n} D}{\mu^{*1/n} q^{1/(3n-2)}}, \end{aligned} \tag{B11}$$

Eq. (B10) reduce to the parametric (in terms of P) solution for all the normalized quantities of (B11) as

$$\begin{aligned} \bar{a} &= C_1^{-1/(3n-2)} [(1/3) + P]^{-n/(3n-2)} P^{1/(3n-2)}, \\ \overline{Rt} &= \bar{a}^2 (1 - 2P/n)/4, \quad \text{and} \quad \bar{D} = (\bar{a}^2 P/C_1)^{1/n} \end{aligned} \tag{B12}$$

From these equations, we can plot $\bar{a} - \overline{Rt}$ (and $\bar{D} - \overline{Rt}$) diagrams for $n \neq 2/3$ (see Figs. 3 and 5).

Asymptotic analyses, based on the solutions of Eq. (B5) in the respective limits $a \to 0^+$ and $a \to +\infty$, show that, depending on which case, and depending on whether $n > 2/3$ or $n < 2/3$, P tends to either 0 or infinity in the limit, and Eq. (B5) is balanced in the limit by either using 1/3 or P on the right side; the other is negligible compared to the one retained.

Equation (B7) indicates $Rt = 0$ when $a = 0$ or $P = n/2$. When $n \neq 2/3$, the latter condition is equivalent to

$$Rt = 0 \quad \text{when } a = a_0 \equiv \left[\frac{6 n^{1/n} C}{2^{1/n} (3n + 2)} \right]^{n/(3n-2)}, \tag{B13}$$

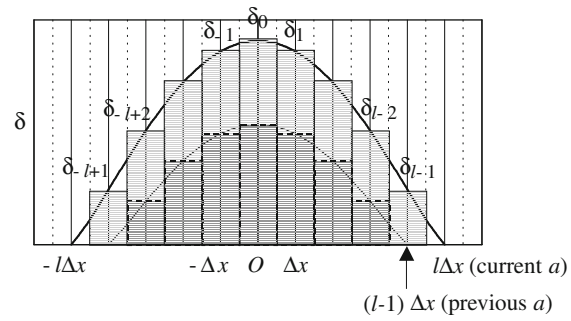

Fig. 11 Illustration of the numerical procedure

or in a normalized form,

$$\overline{Rt} = 0 \quad \text{when } \bar{a} = \bar{a}_0 \equiv \left[\frac{6^n n}{2(3n + 2)^n C_1} \right]^{1/(3n-2)}. \tag{B14}$$

If $n > 1$, $da/d(Rt) = 0$ (and $da/dD = 0$) when $P = P_u \equiv 1/(3n - 3)$. This situation gives a maximum allowable half-length of the slipping region, a_u. Note that $P_u > P_c$ always holds for all $n > 1$. This relation implies, if a becomes larger with the increasing remote loading, the instability of the fault rupture occurs before the slipping region reaches the maximum allowable length. This maximum value terminates the branch of unstable equilibrium states beginning at the critical length, and it is given by

$$a_u = \left[\frac{(3n - 3)^{n-1} C^n}{n^n} \right]^{1/(3n-2)}, \tag{B15}$$

or in a normalized form as

$$\bar{a}_u = \left[\frac{(3n - 3)^{n-1}}{n^n C_1} \right]^{1/(3n-2)}. \tag{B16}$$

B2 The case n=n_{th}(= 2/3)

The case $n = 2/3$ (Fig. 4) is transitional. In this case, $C_1 = 2/3$ and

$$\begin{aligned} C &= (3/2)^{3/2} q^{1/2}, \\ Rt &= (1 - 3P) \kappa a^2/4, \\ D &= [3\kappa P/(2A)]^{3/2} a^3, \end{aligned} \tag{B17}$$

for all a with

$$C P^{3/2} = (1/3) + P. \tag{B18}$$

Or, defining the normalized parameters,

$$\begin{aligned} \bar{a} &\equiv \kappa^{1/2} a/\mu^{*1/2}, \\ \overline{Rt} &\equiv Rt/\mu^*, \quad \text{and} \\ \bar{D} &\equiv A^{3/2} D/\mu^{*3/2}, \end{aligned} \tag{B19}$$

we have

$$\begin{aligned} \overline{Rt} &= \bar{a}^2 (1 - 3P)/4, \\ \bar{D} &= (\bar{a}^2 P/C_1)^{3/2}, \end{aligned} \tag{B20}$$

with

$$(3/2)^{3/2} q^{1/2} P^{3/2} = (1/3) + P, \tag{B21}$$

and q now being $q = \kappa \mu^{*2}/A^3$. This equation shows that P is independent of a; its constant value depends on C of Eq. (B6).

Equation (B17) indicates that Rt is directly proportional to κa^2, with a proportionality constant that is positive (permanently stable growth) if the dimensionless parameter $P < P_c$ and negative (permanently unstable) if $P > P_c$, with $P_c = 1/3$ also satisfying Eq. (B8). From Eq. (B21), we can see that this critical value $P_c = 1/3$ corresponds to $q = q_c$ (= 32/9), and then Eqs. (B17) show that there is a family of solutions (i.e., coordinated pairs D and a) all of which correspond to a fixed tectonic load level $Rt = 0$.

Appendix C Nonlinear slip-weakening: numerical approach

Consider the equilibrium condition for the power-type slip-weakening fault, derived from Eqs. (2, 4, A1 and A2)

$$-A\delta(x)^n = Rt - q(x) - \frac{\mu^*}{2\pi} \int_{a_-}^{a_+} \frac{d\delta(\xi)/d\xi}{x - \xi} d\xi. \tag{C1}$$

In the case that $q(x)$ is of a quadratic form, $q(x) = \kappa x^2/2$, $a_+ = -a_- \ [\equiv a]$ and by employing the simplest discretization method, Fig. 11, with piecewise constant slip in cells of uniform size, we can discretize Eq. (C1) as

$$\begin{aligned} -A\delta(i\Delta x)^n &= Rt - q(i\Delta x) \\ &\quad - K_{ij}\delta(j\Delta x), \quad (-l \le i, j \le l). \end{aligned} \tag{C2}$$

Here l is a positive integer, satisfying $l\,\Delta x = a$ with the uniform grid spacing Δx, $K_{ij} = -\mu^*/\{2\pi\Delta x[(i - j)^2 - 0.25]\}$, and the summation convention is used when there are repeated indices. Note that $\delta(l\Delta x) = \delta(-l\Delta x) = 0$ and from Eq. (C2)

$$Rt = q(l\Delta x) + K_{lj}\delta(j\Delta x), \quad (-l + 1 \le j \le l - 1) \tag{C3}$$

holds, that being the discretized equivalent of the condition of no stress singularity, but rather continuity of stress, at the ends of the slipping zone. In order to determine the stress level, Rt, and the slip distribution, $\delta_i \equiv \delta(i\Delta x)(-l + 1 \le i \le l - 1)$, for the given $a = l\Delta x$, we first eliminate Rt using Eqs. (C2 and C3), and define

$$\begin{aligned} &f_i(\delta_{-l+1}, \delta_{-l+2}, \ldots, \delta_{l-2}, \delta_{l-1}) \\ &\quad \equiv A\delta_i^n + q(l\Delta x) - q(i\Delta x) - (K_{ij} - K_{lj})\delta_j, \\ &\quad (-l + 1 \le i, j \le l - 1) \end{aligned} \tag{C4}$$

and the Jacobian matrix

$$\begin{aligned} J_{ij} &\equiv \partial f_i/\partial\delta_j = nA\delta_j^{n-1}\delta_{i,j} - K_{ij} \\ &\quad + K_{lj}, \quad (-l + 1 \le i, j \le l - 1) \end{aligned} \tag{C5}$$

where $\delta_{i,j}$ is 1 if $i = j$ and 0 if $i \ne j$. Then, the solutions δ_i of $f_i = 0 (-l + 1 \le i \le l - 1)$ can be found by employing the Newton–Raphson method: We start our calculation with the initial values adopted from the known vector $\delta_i(-l + 2 \le i \le l - 2)$ obtained for $a = (l - 1)\Delta x$. Assume $\delta_{-l+1} = \delta_{l-1} = \delta_{l-2}$, and then calculate the correction vector $\Delta\delta_i$ by solving the following simultaneous equations

$$J_{ij}\Delta\delta_j = -f_i. \quad (-l + 1 \le i, j \le l - 1) \tag{C6}$$

We add that correction vector $\Delta\delta_i$ to the initial vector $\delta_i(-l + 1 \le i \le l - 1)$. Iterate the procedure using the modified δ_i until convergence is achieved, i.e., until the maximum value of $|\Delta\delta_i|$ becomes smaller than the allowable error, ε.

References

Abercrombie RE, Rice JR (2005) Can observations of earthquake scaling constrain slip weakening?. Geophys J Int 162(2): 406–424. doi:10.1111/j.1365-246X.2005.02579.x

Ampuero JP, Rubin AM (2008) Earthquake nucleation on rate and state faults—aging and slip laws. J Geophys Res 113:B01302. doi:10.1029/2007JB005082

Bilby B, Eshelby JD (1968) Dislocations and the theory of fracture. In: Liebowitz H (ed) Fracture, an advanced treatise, vol. 1. Academic Press, New York, pp 99–182

Dieterich JH (1979) Modeling of rock friction—1 Experimental results and constitutive equations. J Geophys Res 84:2161–2168

Dieterich JH (1986) A model for nucleation of earthquake slip. In: Das S, Boatwright J, Scholz CH (eds) Earthquake source mechanics, geophysical monograph 37 (Maurice Ewing volume 6), (Am Geophys Union, Washington, DC), pp 37–47

Dieterich JH (1992) Earthquake nucleation on faults with rate- and state dependent friction. Tectonophysics 211:115–134

Dieterich JH, Kilgore BD (1996) Implications of fault constitutive properties for earthquake prediction. Proc Natl Acad Sci USA 93:3787–3794

Lapusta N, Rice JR (2003) Nucleation and early seismic propagation of small and large events in a crustal earthquake model. J Geophys Res 108(B4):2205. doi:10.1029/2001JB000793

Madariaga R (1976) Dynamics of an expanding circular fault. Bull Seismic Soc Am 66:639–666

Noda H, Dunham EM, Rice JR (2009) Earthquake ruptures with thermal weakening and the operation of major faults at low overall stress levels. J Geophys Res 114:B07302. doi:10.1029/2008JB006143

Rice JR (1992) Dislocation nucleation from a crack tip: an analysis based on the Peierls concept. J Mech Phys Solids 40:239–271

Rice JR, Beltz GE (1994) The activation energy for dislocation nucleation at a crack. J Mech Phys Solids 42:333–360

Rice JR, Uenishi K (2002) Slip development and instability on a heterogeneously loaded fault with power-law slip-weakening. Eos Trans. AGU, 83(47), Fall Meet Suppl, Abstract S61E-06

Rubin AM, Ampuero J-P (2005) Earthquake nucleation on (aging) rate and state faults. J Geophys Res 110:B11312. doi:10.1029/2005JB003686

Ruina A (1983) Slip instability and state variable friction laws. J Geophys Res 88:10,359–10,370

Tse ST, Rice JR (1986) Crustal earthquake instability in relation to the depth variation of frictional slip properties. J Geophys Res 91:9452–9472

Uenishi K, Rice JR (2003) Universal nucleation length for slip-weakening rupture instability under nonuniform fault loading. J Geophys Res 108(B1):2042. doi:10.1029/2001JB001681

Uenishi K, Rice JR (2004) Three-dimensional rupture instability of a slip-weakening fault under heterogeneous loading. Eos Trans. AGU, 85(46), Fall Meet Suppl, Abstract S13E-04

Uenishi K, Rice JR (2010) Three-dimensional rupture instability of a displacement-softening interface under heterogeneous loading (to be submitted)